

Search for high-energy photons and neutrinos, producing air showers with energy above 10^{18} eV by the Yakutsk array data.

Igor Petrov*

Yu.G. Shafer Institute of Cosmophysical Research and Aeronomy

E-mail: igor.petrov@ikfia.ysn.ru

Stanislav Knurenko

Yu.G. Shafer Institute of Cosmophysical Research and Aeronomy

E-mail: knurenko@ikfia.ysn.ru

Zim Petrov

Yu.G. Shafer Institute of Cosmophysical Research and Aeronomy

E-mail: pze@ikfia.ysn.ru

Yuri Egorov

Yu.G. Shafer Institute of Cosmophysical Research and Aeronomy

E-mail: zeppelin@ikfia.ysn.ru

A complex analysis of the data of the Yakutsk array has been carried out to search for primary photons that generate extensive air showers with energies above 10^{18} eV. Within the framework of the integrated approach, a sample of showers with energies above 10^{19} eV and zenith angles $\theta \geq 60^\circ$ is separately considered to search for EAS produced by neutrinos. On the basis of calculations and experimental data, selection criteria were constructed and samples were sampled by these criteria for showers close in their characteristics to showers formed by primary photons. According to these data, the upper limit of the primary photon flux in the cosmic radiation of the limiting energies is estimated.

*35th International Cosmic Ray Conference - ICRC2017-
12-20 July, 2017
Bexco, Busan, Korea*

*Speaker.

1. Introduction

The nature of generation of cosmic rays of ultrahigh energies (above 10^{18} eV) in the Universe is still unknown [1, 2]. According to models [3-5], primary photons of high and ultrahigh energies and astrophysical neutrinos are expected to exist in cosmological space, along with other particles (nuclei of various chemical elements). The expected flux of cosmic rays of ultrahigh energies, near the Earth, will depend on nature, the degree of propagation and spatial distribution of astrophysical sources [6, 7].

Photons do not deflect from their original direction because its charge is neutral and for this reason are good for searching point sources generating ultra-high energy particles. For this reason, the photon component can be used to determine the physical characteristics of cosmic ray sources and study the interaction of primary photons of ultrahigh energy with the photon field of the Universe and, as a consequence, to explain the shape of the cosmic-ray spectrum in the energy range 10^{19} - 10^{20} eV [8-12].

Neutral particle produced air showers due to their physical properties can go a long way in the matter and their depth of the maximum development near sea level, i.e. "young showers". The base of such air shower is electron-photon component, which scatters to big angles and has big delay relative to particles in the shower core. Hence, in such shower events one needs to expect a large number of peaks from electrons, positrons and photons on the signal scan from scintillation detector [13 - 15].

2. Primary ultra-high energy gamma quants and astro-neutrino search methodology.

2.1 The Yakutsk array detectors.

At the Yakutsk array for registration, charged particles standard scintillation detectors with area $s = 2 \text{ m}^2$ and threshold $\varepsilon_{thr.} \geq 10 \text{ MeV}$ is used. There are also detectors with $s = 1 \text{ m}^2$ and threshold $\varepsilon_{thr.} \geq 1.8 \text{ MeV}$. Structure and data about detectors are shown in Fig. 1. There are, also, Cherenkov light detectors which located near central station at the area of $s = 1 \text{ km}^2$. At the Yakutsk array, also differential detectors, or tracking Cherenkov detectors, are used to register the longitudinal development of the EAS. These are detectors with a good time resolution for measuring the flux of Cherenkov photons arriving from a narrow region in height [14].



Figure 1: The Yakutsk array detectors: the structure of scintillation detector with area 2 m^2 (left), new scintillation detector with area 1 m^2 (middle), muon detectors stations with a threshold 1 GeV (right)

The registration of muons is carried out by similar detectors installed in underground stations under a layer of the ground of thickness $l = 2.4 \text{ m}$. The muon detectors are placed at different

distances from the center of the array. In the center of the array is a large muon detector with a threshold of 0.5 GeV and an area of $s = 190 \text{ m}^2$. At distances of 500 m, 800 m and 1000 m there are three detectors with thresholds of 1 GeV and $s = 20 \text{ m}^2$ each. The photo of the muon station is shown in Fig. 1. In the stations there are 10 scintillation detectors with $s = 2 \text{ m}^2$ each and electronics. Such stations are designed to measure the amplitude of the signal from the scintillation detector. Communication with the central station is carried out via cable. All stations work as an independent unit and the data transferred to the main central station when "master" trigger signal is produced by the central station.

3. Experimental data

3.1 Longitudinal development of air showers: depth of maximum development X_{max}

Longitudinal development of the shower at the Yakutsk array is reconstructed by the data of registration of the Cherenkov light [15, 16], using the mathematical apparatus used in solving inverse problems [17, 18]. Fig. 3 shows the dependence of X_{max} from classification parameter Q (200).

Using the database of Cherenkov data, the distribution of X_{max} from the primary energy of the shower was obtained (see Fig. 3). It can be seen from Fig.3 that in the distribution there are cases of EAS with $X_{max} \geq 800 \text{ g / cm}^2$, i.e. have a low maximum development of the shower in relation to the events formed by the iron nucleus and even the proton. These showers formed the basis for this analysis.

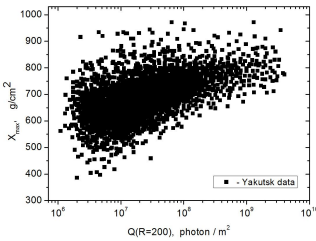


Figure 2: Dependence of X_{max} from classification parameter Q (200) - EAS Cherenkov light flux density at a distance of 200 m from the shower axis. Data obtained in 1973-2014.

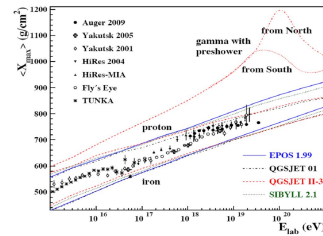


Figure 3: Dependence of X_{max} from energy. Experimental data comparison with calculations for different hadron interaction models (proton, iron nuclei and high-energy gamma ray). Data obtained in 1973-1993 [19]

The averaged data of the Yakutsk array together with the data of other array are shown in Fig. 3. There also calculations are made for some models of hadronic interactions for primary nuclei and high-energy gamma quantum. As can be seen from Fig. 3, the air shower from the gamma-ray quantum has X_{max} of (150-180) g / cm^2 lower in the atmosphere than in a proton with an energy of 10^{19} eV. In fact, cascade curve X_{max} from gamma ray is near sea level at depth $\sim 950 \text{ g/cm}^2$. In this case, there is a narrow cascade mainly consisting of electrons and photons with a very low content of muons. This distinguishes shower produced by gamma ray from shower produced by proton or

nucleus of any other element. We can assume that X_{max} can be used as the first criterion to search for EAS produced by gamma ray.

3.2 Amount of muons in air showers

Gamma ray produced shower consist small number of muons. If the array detects muons then on number of muons in the shower one can judge the nature of the primary particle i.e. its atomic weight. We can assume this from calculations of muon components by hadron interaction models shown in Fig. 4 and 5 [20, 21].

At the Yakutsk array the proportion of muons in the shower determined by relation of muon flux density at distances of 600m and 1000m to the total charged component $\rho_\mu/\rho_{\mu+e}$, since these parameters are measured with better accuracy than the total number of muons N_μ and charged particles $N_{\mu+e}$ in showers with total energy $E_0 \geq 10^{18}$ eV. This will be the second criterion to search showers produced by neutral particles that includes gamma rays and neutrino.

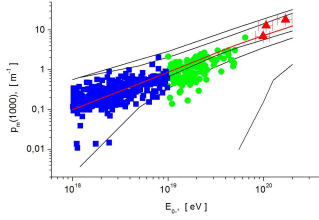


Figure 4: Energy dependency of $\rho_\mu(1000)$ for observed events with energy 10^{18} - 10^{19} eV (squares) and 10^{19} - 10^{20} eV (triangles). Expected $\pm 1\sigma$ bounds of the distributions are indicated for proton, iron and gamma by different curves

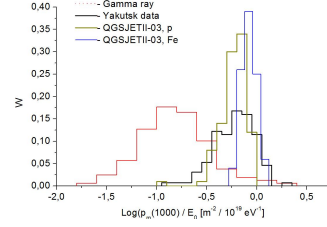


Figure 5: Fluctuations of $\rho_\mu(1000)/10^{19}$ value (eV) in showers with $E_0 > 10^{19}$ eV compared to simulation results (QGSjetII-03 + UrQMD) for proton, iron and photon

Fig. 4 shows that there is overlapping region for gamma ray calculations (solid line) and the experimental data. In Fig. 5 there is also similar overlap, which shows muon flux fluctuations at distance 1000 m from shower axis, normalized to the shower energy (dots). This suggests the existence of high-energy gamma rays in the flow of cosmic particles, which produces EAS in the Earth's atmosphere.

Fig. 6 shows the calculations of the relative muon content in the EAS using the muon flux density at a distance of 600 m from the shower axis. Calculations are performed for the primary gamma quantum, proton and iron nucleus. It is seen from Fig. 6 that the average distribution of each of the components of CR is localized in a certain region and can be distinguished in the experiment with good accuracy of muon measurements. As can be seen from the calculation, in air showers produced by gamma-quantum the content of muons is much smaller than in the shower produced by the proton and at a measurement accuracy of $\rho_\mu(600) = 5$ - 10% , it is not difficult to find out the EAS produced by the gamma quantum. Such work is planned in the near future at the Yakutsk installation.

It's well known that muon number depends on the height of maximum development of air showers in the atmosphere. That is why a fraction of muons very sensitive to X_{max} of cascade curve.

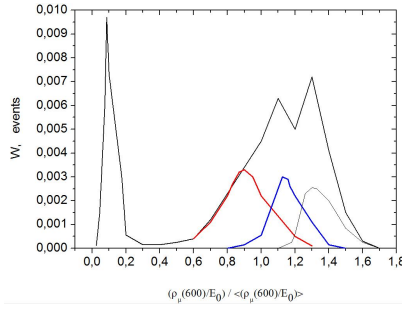


Figure 6: Distribution of showers with energy above 10^{18} eV and zenith angles of 0° to 70° . The curves for the gamma-quantum, proton, carbon, and iron nucleus are calculated using the QGSjetII-03 model.

This follows from calculations based on the QGSjetII-04 model. And the fraction of muons from the proton and iron nucleus, as it follows from Fig. 7, is localized in different places, which makes it possible to divide showers into protons and showers from the iron nucleus in this parameter. And that feature was used in the present paper to search for neutral particles in cosmic rays.

For this, we used the experimental dependence of X_{max} on $\rho_\mu(600)/\rho_s(600)$, shown in Fig.7. There also calculations are made for the model QGSjetII-04 for different zenith angles (Fig. 8). The agreement of calculations with experiment indicates that the model QGSjetII-03, after its modernization, is close to the description of the experiment on the muon component and the problem of muon deficit is gradually being solved.

3.3 Dependence of muon fraction on X_{max}

It's well known that muon number depends on the height of maximum development of air showers in the atmosphere. That is why a fraction of muons very sensitive to X_{max} of cascade curve. This follows from calculations based on the QGSjetII-04 model. And the fraction of muons from the proton and iron nucleus, as it follows from Fig. 7, is localized in different places, which makes it possible to divide showers into protons and showers from the iron nucleus in this parameter. And that feature was used in the present paper to search for neutral particles in cosmic rays.

For this, we used the experimental dependence of X_{max} on $\rho_\mu(600)/\rho_s(600)$, shown in Fig.7. There also calculations are made for the model QGSjetII-04 for different zenith angles (Fig. 8). The agreement of calculations with experiment indicates that the model QGSjetII-03, after its modernization, is close to the description of the experiment on the muon component and the problem of muon deficit is gradually being solved.

3.4 Signal time sweep of surface and underground scintillation detectors. Signals from electron and muon components. Number of peaks.

Air showers produced by different primary particles have a maximum development at different depth in the atmosphere. Because of this, part of secondary particles (mostly electrons) loses energy to ionization of the air and eliminated from the cascade process. Then on the sea level will arrive a certain type of particles: electrons, photons, muons in the case of inclined shower and only muons in the case of strongly inclined showers, which can be seen in the signal time sweep of scintillation detectors. For the primary gamma ray and neutrino, depth of maximum is going to

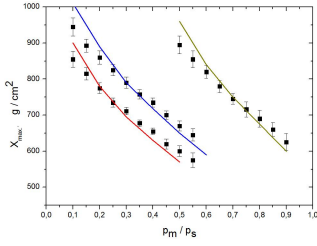


Figure 7: Dependence of muon fraction on depth of maximum development of electron-photon cascade of air showers at zenith angles $\theta_1 = 18^\circ$, $\theta_2 = 38^\circ$ and $\theta_3 = 58^\circ$. Experimental data.

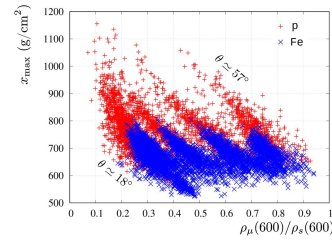


Figure 8: Dependence of relative muon fraction with $\epsilon_{thr.} \geq 1$ GeV on the depth of maximum development. Calculation made on QGSjetII-04 model for protons and iron nucleus for different zenith angles.

be near the level of observation and we can expect scintillation detector response inherent in the electron-photon component of the shower. This is another criterion by which we can select showers produced by neutral particles.

Examples of scintillation detector responses in the case of vertical and inclined showers are given in Fig. 9 and Fig. 10. Fig. 9 and Fig. 10 shows that the shape of the pulse in each case is different. Vertical showers have many peaks, where each peak corresponds to a group or a single particle. As can be seen, all of the particles are distributed in time, i.e. they arrive with different delays with respect to the first particle. Most likely, it is the electrons scattered in the shower subcascades.

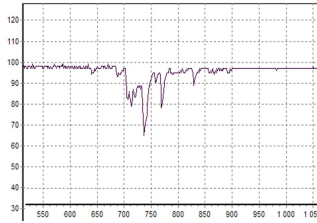


Figure 9: Vertical air shower pulse. $E_0 = 1.7 \cdot 10^{19}$ eV, $\theta = 18^\circ$, $R = 1298$ m. Detector with area $s = 2$ m² and threshold $\epsilon_{thr.} \geq 10$ MeV

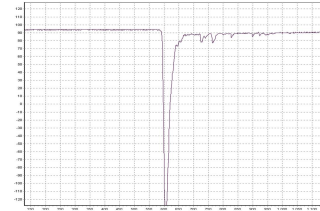


Figure 10: Inclined air shower event. $E_0 = 2.4 \cdot 10^{19}$ eV, $\theta = 56^\circ$, $\psi = 200^\circ$, $R = 1000$ m.

From Fig. 9 it is seen that in strongly inclined showers the pulse structure is different from vertical showers. It is clear single and narrow pulse. The compactness of the arrival of these particles indicates that these particles are produced in the first interactions of primary particle with air nuclei and in the course of decay processes of π^\pm - mesons, i.e. they are muons.

4. Experimental data analysis

4.1 Estimation of gamma-rays flux upper limit

To search for ultrahigh-energy gamma rays, showers were analyzed for the period from 2000

Table 1: Air shower events, possibly produced by primary gamma rays

Date	Time	$\lg E_0$	θ , deg	$\rho_\mu / \rho_{\mu+e}$	X_{max} , g/cm ²	n, num. of peaks
05.03.2002	23:34:18	19.70	44.2	0.24±0.06 (0.17)	837	3
07.12.2005	01:11:45	19.28	32.4	0.18±0.05 (0.15)	871	4
24.01.2006	19:03:59	19.41	10.9	0.08±0.03 (0.08)	947	7
11.05.2007	06:23:31	19.35	9.9	0.09±0.04 (0.09)	909	6
08.05.2008	20:36:02	19.18	19.8	0.15±0.04 (0.14)	897	5
13.03.2010	16:36:00	19.60	23.9	0.11±0.03 (0.10)	915	7
24.01.2006	19:03:59	19.41	10.9	0.08±0.06 (0.08)	864	6

to 2014. Four energy intervals were examined in each of which the search for EAS events satisfying the above described criteria was carried out. The showers selected in this way formed the basis for further analysis. As an example, Table. 1 shows the characteristics of some of the selected showers

For analysis, the time interval 2000 - 2014 was taken and the energy range $1 \cdot 10^{18} - 5 \cdot 10^{19}$ eV is considered. The entire energy range was divided into energy intervals equal to $1 \cdot 10^{18} - 3 \cdot 10^{18}$ eV, $3 \cdot 10^{18} - 6 \cdot 10^{18}$ eV, $6 \cdot 10^{18} - 9 \cdot 10^{18}$ eV, $9 \cdot 10^{18} - 50 \cdot 10^{18}$ eV. For better sampling efficiency, showers were sampled at the center of the array in an area of $s = 3$ km² to energies up to $6 \cdot 10^{18}$ eV, and above this energy in an area $s = 12$ km². In this case, the probability of registering showers was higher than $W \geq 0.9$ and the accuracy of the EAS parameters being determined was not worse than 15%. When searching for showers of EAS candidates from the primary gamma quantum, the above-described criteria for characteristics such as X_{max} , ρ_μ / ρ_s and the number of peaks in the signals of scintillation detectors of ground and underground placement were taken into account. Further, by the formula (4.1) was calculated F_γ^{95CL} :

$$F_\gamma^{95CL} = (N_\gamma^{95CL}(E_\gamma > E_0)) / \varepsilon_{\gamma,min} \quad (4.1)$$

where E_γ - photon energy, N_γ^{95CL} - the number of air showers above E_0 at 95 % confidential level, the candidates produced by primary gamma-rays, $\varepsilon_{\gamma,min}$ - Cherenkov and scintillation detectors operation time at the Yakutsk array.

Upper limit for flux of primary gamma rays for each of intervals: 1. $\langle E_0 \rangle = 1 \cdot 10^{18}$ eV, $F_\gamma^{95CL} = 8.3 \cdot 10^{-2}$; 2. $\langle E_0 \rangle = 3 \cdot 10^{18}$ eV, $F_\gamma^{95CL} = 4.9 \cdot 10^{-2}$; 3. $\langle E_0 \rangle = 6 \cdot 10^{18}$ eV, $F_\gamma^{95CL} = 1.2 \cdot 10^{-2}$; 4. $\langle E_0 \rangle = 9 \cdot 10^{18}$ eV, $F_\gamma^{95CL} = 6.9 \cdot 10^{-3}$ [km⁻²sr⁻¹y⁻¹].

Thus, according to the data of the Yakutsk array, the upper limit of the integral photon flux I_γ was higher than 1 EeV, up to 10 EeV. The present results, together with the data of the Auger [41, 42], TA [43] and the earlier data of the Yakutsk array [44], are shown in Fig. 11. Comparing the limits of the flux of gamma rays with the Yakutsk spectrum at the appropriate energies, the upper limit of the fraction of photons was 0.4% at an energy of 1 EeV and 8.0% at 10 EeV.

These estimates can be affected by the following inaccuracies in measurements: 1. Errors in the estimation of X_{max} , at the Yakutsk array, the accuracy of the determination of X_{max} is ± 25 g / cm². 2. Errors in the log of the shower axis, especially near the array boundary, according to $X_0 = 25$ m, $V_0 = 35$ m. 3. Uncertainty in estimating the energy of the shower by the energy

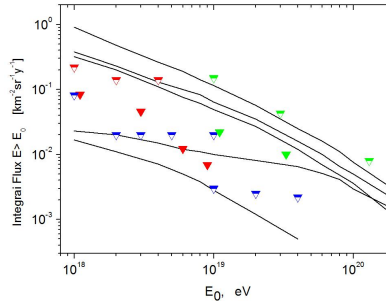


Figure 11: Upper limit of primary photons of CR flux by the Yakutsk array (red triangles). Auger (blue triangles) [22,23], AGASA [24], Telescope Array (green triangles) [25] and "top-down" prediction for the following sources: super heavy dark matter (dash[26] and dash dot dot [27]), topological defects [26] (dot), Z-bursts [26] (dash dot).

balance method $\sim 25\%$ [28]. The results obtained in this paper can be regarded as an indication of the possible existence in the cosmic ray flux of ultrahigh-energy gamma rays.

5. Conclusion

Long-term, continuous observations of the EAS at the Yakutsk array made it possible not only to study the processes of interaction and development of cascades of various particles in the atmosphere but also directly to search for such neutral particles as photons of ultrahigh energies and astrophysical neutrinos.

Multi component analysis of air showers with the use of above described criteria, found no showers produced by gamma ray or neutrino [30]. At the same time, QGSJETII-03 model calculations for the primary protons and iron nuclei and gamma ray [31] (Fig. 3, Fig. 4 and Fig. 5) tells that if fluctuations of the muon measurements within 1σ is taken into account, the probability of detecting air shower produced by neutral particles exist. "Muonless" showers detected at the Yakutsk array and selected in the current work (Table 1) can be considered as candidates for such showers [32].

The presented results (Fig. 11) on the upper limit of the gamma ray flux can be used to test various astrophysical models (including the search for dark matter) and to establish the nature of the formation of particles such as astro-neutrinos in cosmological space.

In order to study the nature of neutral particles in the region of ultrahigh energies, it is required to improve the method of registration, first of all, of strongly inclined showers. It is even possible to create specialized arrays, for example, muon telescopes of a large receiving area for registering the muon fraction with an accuracy of 3-5% in individual EAS events.

Acknowledgments

The reported study was funded by RFBR according to the research project 16-29-13019.

References

- [1] P. Bhattacharjee, G. Sigl. Phys. Rev. **327**, 109 (2000)

- [2] F. Halzen & D. Hooper. Rep. Prog. Phys. **65**, 1025(2002).
- [3] J.K. Becker. Phys. Rep. **458**, 173 (2008).
- [4] M. Ahlers et al. Astropart. Phys. **34**, 106 (2010).
- [5] K. Kotera et al. JCAP. **10**, 013 (2010).
- [6] G. Gelmini, O. Kalashev, D. Semikoz. // J. Theor. Phys. **106**, 1061 (2008).
- [7] K. Greisen, Phys. Rev. Lett. 16 (1966) 748. G.T. Zatspin, V.A. Kuzmin, JETP Lett. **4**, 78 (1966).
- [8] K. Shinozaki et al. Astrophys. J. **571**, L117 (2002).
- [9] M.Ave et al. Phys. Rev. Lett. **85** (2000)
- [10] M. Risse et al. Phys. Rev. Lett. **95**, 171102(2005).
- [11] The Pierre Auger Collaboration. Astropart. Phys. **31**, 399(2009).
- [12] Stanislav Knurenko, Zim Petrov and Yuri Yegorov. J. Phys.: Conf. Ser. **409** 012090(2013).
- [13] S. Knurenko, A. Sabuorov. Proceedings of the 33th International Cosmic Ray Conference, Rio-de-Janeiro, 2013, paper ID 0055.
- [14] M.N. Dyakonov, S.P. Knurenko, V.A. Kolosov et al. Nuclear Instruments and Meth-s in Phys. Rec. Amst., A248 (1986), v.4, p. 224-226.
- [15] Knurenko S.P., Kolosov V.A., Petrov Z.E. // Proc. 27-th ICRC, Hamburg (Germany), v.1, p.157-160 (2001).
- [16] G.K. Garipov, V.M. Grigoryev, N.N. Efremov et al. Proceedings of ICRC, p. 885-887 (2001).
- [17] Knurenko S.P, Kolosov V.A., Petrov Z.E, et al. // Proc. 27th ICRC, Hamburg, v.1 (2001).
- [18] A.N. Tikhonov, V. Ya. Arsenin. Moscow: Science, 286 (1979).
- [19] Dyakonov M.N., Ivanov A.A., Knurenko S.P. et al. // Proc. 23sd ICRC, Calgary, v.4 (1993).
- [20] S.P. Knurenko et al. // Nuclear Physics B (Proc. Suppl.) 151, 92-95 (2006).
- [21] S.P. Knurenko, A.A. Ivanov, M.I. Pravdin, A.V. Sabourov, and I.Ye. Sleptsov. Nucl. Phys. B (Pros. Suppl.), 175-176, p. 201 – 206 (2008).
- [22] S.P. Knurenko, A.V. Sabourov. // Nuclear Physics B (Proc. Suppl.) 196, 319-322 (2009).
- [23] M. Settimo for the Pierre Auger Collaboration. 32nd ICRC, Beijing (China). 393 (2011). arXiv: 1107.4805 [astro-ph.HE].
- [24] V. Scherini for the Pierre Auger Collaboration. EPJ Web of Conferences 53, 05002 (2013). DOI: 10.1051/epjconf/20135305002.